The Exact and Statistical Studies on Unsteady Rotating Second Grade Fluid through Riga Plate

Ahmad Qushairi Mohamad
Department of Mathematical Sciences, Faculty of Science, Universiti Teknologi Malaysia

Zakaria, Nordin
Department of Computer and Information Sciences, Universiti Teknologi PETRONAS

Shafie, Sharidan
Department of Mathematical Sciences, Faculty of Science, Universiti Teknologi Malaysia

Khan, Ilyas
Department of Mathematics, College of Science Al-Zufi, Majmaah University

他

https://doi.org/10.5109/7395663

出版情報：Proceedings of International Exchange and Innovation Conference on Engineering & Sciences (IEICES). 11, pp.1198-1205, 2025-10-30. International Exchange and Innovation Conference on Engineering & Sciences
バージョン：

The Exact and Statistical Studies on Unsteady Rotating Second Grade Fluid through Riga Plate

Ahmad Qushairi Mohamad[1], Nordin Zakaria[2], Sharidan Shafie[1], Ilyas Khan[3], Dumitru Vieru[4]
[1]Department of Mathematical Sciences, Faculty of Science, Universiti Teknologi Malaysia, 81310, Johor Bahru, Johor, Malaysia,
[2]Department of Computer and Information Sciences, Universiti Teknologi PETRONAS, Seri Iskandar, 32610, Perak, Malaysia,
[3]Department of Mathematics, College of Science Al-Zufi, Majmaah University, Al-Majmaah, 11952, Saudi Arabia,
[4]Department of Theoretical Mechanics, Technical University of Iasi R-6600 Iasi, Romania
Corresponding author: ahmadqushairi@utm.my

Abstract: *This paper investigates the behavior of second grade fluid in a system involving rotation and a Riga plate. As is well known, second grade fluid is a type of non-Newtonian fluid with exceptionally high viscosity. Therefore, to mitigate the significant effects of this viscosity, rotational and magnetic forces (generated by the Riga plate) are applied to the fluid system, with both forces aligned with the flow direction of the fluid. What is more intriguing is that such a study has never been conducted by other researchers. Hence, this study aims to explore Unsteady Second Grade Fluid through the Riga Plate with the rotation effect, using both analytical and statistical approaches to formulate an initial hypothesis. The governing dimensionless equations, along with the initial and boundary conditions, will be derived based on the Boussinesq approximation assumption and relevant physical diagrams. These equations will then be translated into a dimensionless form using appropriate dimensionless variables. The Laplace transform is subsequently applied to solve the momentum equations and obtain the output velocity profiles. The results will be presented graphically to examine changes in velocity as a function of the involved parameters. The Response Surface Methodology (RSM) is employed to identify the dominant and optimum rotational or magnetic parameters in determining the velocity rate. This study also aims to serve as an important benchmark for future numerical and experimental studies.*

Keywords: Second grade fluid; Riga Plate; Rotating; Laplace transform; Response Surface Methodology

1. INTRODUCTION

Second grade fluids are classified as non-Newtonian fluids because their properties do not conform to Newton's Law of Viscosity, where shear stress is perpendicular to the deformation of velocity. As a result, the viscosity of these fluids is elevated even when high shear stress is applied to their surface. The concept of second grade fluids was introduced by Coleman and Noll in 1960, initially observed in polymer fluids. Their research revealed that these fluids not only possess high viscosity but also exhibit elastic properties, making them viscoelastic fluids. Examples include polymers, honey, and ketchup [1]. In mathematical modeling, second grade fluids are among the most complex to analyze, yet their solutions are invaluable in practical applications, such as blood flow, lubricants, liquid metals, alloys, and paints [2-3].

Given the diverse range of applications, second grade fluids have been extensively studied, particularly in theoretical research. Several studies have explored the impact of rotational forces on viscosity reduction and enhanced fluid movement. Modeling of rotating flow is crucial across a wide range of scientific, engineering, and product design applications, enabling the design of products such as jet engines, pumps, and vacuum cleaners, as well as providing valuable insights for modeling geophysical flows [4]. Pioneers in this area, Hayat and Hutter [5] and Hayat et al. [6], examined the effect of rotation in second grade fluids, considering their electrical conductivity and magnetic effects. In 2005, Hayat et al. [7] extended their work by incorporating the Hall current effect into the magnetic analysis. Later, in 2008, Hayat et al. [8] introduced a porous medium into the model, which increased the complexity of the mathematical equations but sufficiently captured all the body forces in the fluid flow system. These studies were solved analytically using the Laplace transform method, offering a benchmark for validating numerical and experimental approaches.

Building on this foundation, Khan et al. [9] furthered Hayat et al. [8] work by modifying the boundary conditions. They analyzed fluid behavior with constant and variable acceleration boundary conditions, finding that altering these conditions complicated the solution and increased the fluid flow speed compared to static or moving boundaries. Their findings highlighted fluctuating velocity profiles due to the viscous and elastic characteristics of second grade fluids. Expanding on this, Imran et al. [10] and Zafar et al. [11] explored oscillating boundary conditions while focusing on classical and fractional derivatives. Subsequent studies, such as the one by Mohamad et al. [12], investigated new body force effects, such as convection, using the Laplace transform method. However, none of these studies incorporated the Riga plate.

The Riga plate, first discovered by Gailitis and Lielausis as actuators made of alternating magnets and electrodes [13], shares similarities with magnetohydrodynamics (MHD) because it generates Lorentz force through electrically conducting fluids. However, unlike MHD, where the force direction opposes fluid flow, the force generated by the Riga plate aligns with the fluid flow. This unique feature makes the Riga plate crucial for enhancing fluid flow velocity. Its precise control allows for manipulation of fluid flow and force, making it applicable in various industries, including magnetohydrodynamic power generation, flow control, propulsion, and fluid mixing [14-16]. Anjum et al. [17] examined the Riga plate's effect in second grade fluid systems, solving the problem using the approximate homotopic method. Ghulam Rasool et al. [18] extended this research by investigating the impact of nanoparticles under zero mass flux conditions. Their study showed that the Lorentz force generated by the Riga plate exceeded the fluid velocity. Ghulam Rasool et al. [19] continued their research by incorporating Buongiorno's nanofluid model, while Hassan Waqas et al. [20] explored the effects of bio-convection in the presence of the Riga plate, using BVP4C in MATLAB. Additionally, Al-Zubaidi et al. [21] analyzed the behavior of second grade fluid in a squeezing Riga plate using numerical methods. Kotha Gangadhar et al. [22] referenced Ghulam Rasool et al.'s work to study the impact of radiation effects, showing that the flow rate increased with the addition of this effect. Wasfi et al. [23] conducted a new study on second grade fluid in a slandering vertical Riga sheet, also using BVP4C. Other related studies by Najihah et al. [24] and Sohail et al. [25] also used numerical approaches, but none utilized an analytical method to explore the impact of the Riga plate on second grade fluid. Notably, no studies have investigated the effects of rotating second grade fluid in the presence of the Riga plate.

Thus, this study aims to conduct an analytical investigation of unsteady rotating second grade fluid through the Riga plate using the Laplace transform method. It excludes heat effects, nanofluids, and other body forces, opting for a non-moving boundary condition. The goal is to pioneer future research while addressing gaps in previous studies. This study will examine whether the rotation effect, Riga effect, or both enhance second grade fluid movement, as both are forces acting within the fluid system. The physical diagram and Boussinesq approximation assumptions are employed to derive the governing dimensionless equations, along with the initial and boundary conditions. These equations will be translated into a dimensionless form using appropriate variables. The Laplace transform will be applied to solve the momentum equations and obtain velocity profiles, which will be presented graphically to analyze changes in velocity based on the involved parameters. Furthermore, the Response Surface Methodology (RSM), as referenced by Wahid et al. [26] and Abu Bakar et al. [27], will be used to identify the dominant rotational or magnetic parameters for optimizing velocity rates. This study aims to serve as an important benchmark for future numerical and experimental research.

2. RESEARCH METHODOLOGY

The unsteady flow of an incompressible second grade fluid over a Riga plate, considering the effects of rotation, will be modeled by formulating the dimensional partial differential equations for momentum, along with the corresponding initial and Riga-type boundary conditions, extended and derived from Hayat et al. [8]. The Riga plate variable will follow the model proposed by Reyaz et al. [14] and Hakeem et al. [28]. Appropriate dimensionless variables will be introduced to transform the governing equations, initial conditions, and boundary conditions into dimensionless form. Through this process, the relevant dimensionless fluid parameters will be identified.

Subsequently, the Laplace transform method will be applied to solve the resulting equations, yielding exact solutions for the velocity profiles. This technique is considered suitable, as it can be effectively applied to linear equations involving rotating geometries and time-dependent conditions. The exact solutions will be plotted graphically using Mathcad software to analyze the influence of various dimensionless parameters on the velocity profiles.

In addition, numerical values for skin friction will be evaluated and incorporated into a Response Surface Methodology (RSM) framework to assess the optimal influence of fluid parameters on the rate of velocity change. The overall operational framework for the research methodology is illustrated in Figure 1.

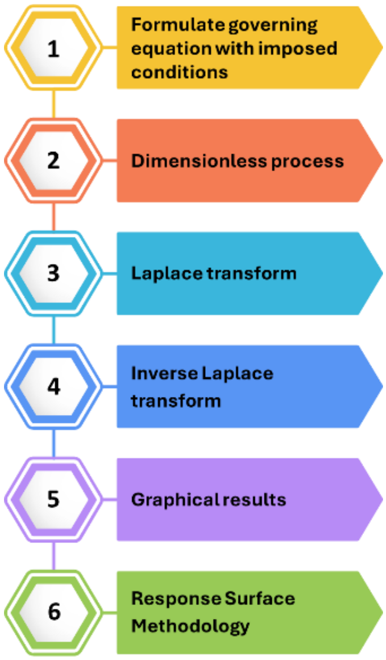

Fig. 1. Operational framework for the research methodology

3. MATHEMATICAL FORMULATION

Consider the unsteady flow of a rotating, incompressible second grade fluid past an infinite vertical Riga plate. The x-axis is oriented upward along the plate, and the z-axis is normal to the plate. Initially, both the plate and the fluid are at rest at time t=0. For t>0t, the fluid begins a solid body rotation with a constant angular velocity Ω parallel to the z-axis, and the Riga plate starts to induce an electromagnetic field. This results in the generation of a Lorentz force, F, which acts upward in the x-direction. The physical setup of the problem is illustrated in Figure 2.

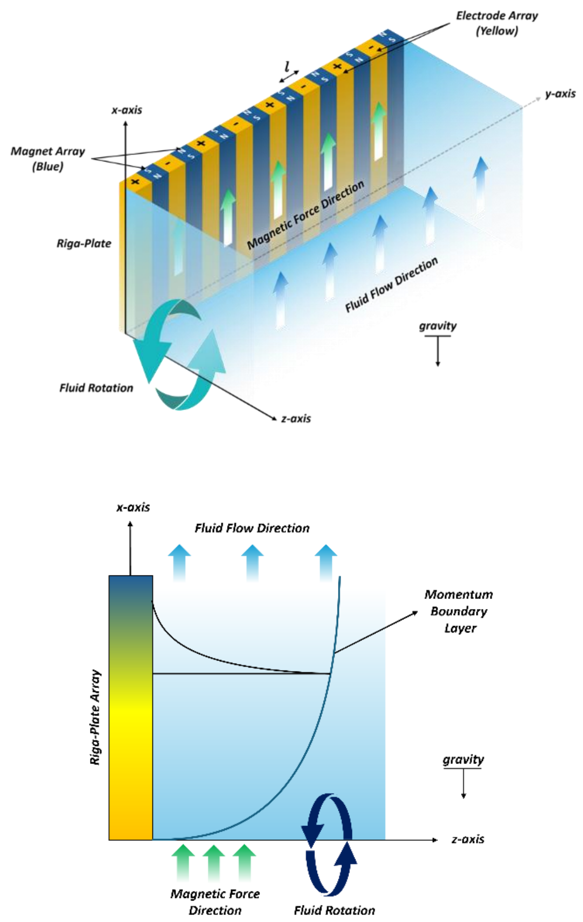

Fig. 2. Physical configuration of the rotating second grade fluid flow through infinite vertical Riga plate

Taking into account the Boussinesq approximation, relevant literature, and the physical configuration and assumptions presented in Figure 2, the governing momentum equation in the form of a partial differential equation (PDE) for this research problem can be formulated as follows [8,14,28]:

$$\frac{\partial F^*}{\partial t^*}+2i\Omega F^* = \upsilon\frac{\partial^2 F^*}{\partial z^2}+\frac{\alpha_1}{\rho}\frac{\partial^3 F^*}{\partial z^2 \partial t} + \frac{\pi J_0 M_0}{8\rho}\exp\left(-\frac{\pi}{l}z\right) \tag{1}$$

together with selected initial and Riga boundary conditions as

$$\begin{aligned} &F^*(z^*,0)=0 \quad ; \quad z^*\ge 0,\\ &F^*(0,t^*)=0 \quad ; \quad t^*>0,\\ &F^*(\infty,t^*)\to 0 \quad ; \quad t^*>0. \end{aligned} \tag{2}$$

Let $F^*=F^*(y,t)=u^*(y^*,t^*)+iv^*(y^*,t^*)$ be the complex velocity, $u^*(y^*,t^*)$ the primary velocity, and $v^*(y^*,t^*)$ the secondary velocity. Let i denote the imaginary unit, υ the kinematic viscosity, α_1 the second grade fluid parameter, ρ the fluid density, J_0 the applied current density, M_0 the magnitude of magnetization of the magnets, and l the length of the electrodes and magnets. Equations (1) and (2) are presented in dimensional form, expressed using SI units. Therefore, to eliminate the units and transform the governing equations into a dimensionless form, suitable dimensionless variables are introduced and defined as follows:

$$F=\frac{F^*}{U_0}, \qquad z=\frac{U_0}{\nu}z^*, \qquad t=\frac{U_0{}^2}{\nu}t^*. \tag{3}$$

Thus, by substituting the dimensionless variables from equation (3) into equations (1) and (2), the dimensionless momentum equations and boundary conditions can be obtained as follows:

$$\frac{\partial F}{\partial t}+2i\omega F=\frac{\partial^2 F}{\partial z^2}+\alpha\frac{\partial^3 F}{\partial z^2\partial t}+E\exp(-lz) \tag{4}$$

and

$$\begin{aligned} &F(z,0)=0 \quad ; \quad z\ge 0,\\ &F(0,t)=0 \quad ; \quad t>0,\\ &F(\infty,t)\to 0 \quad ; \quad t>0, \end{aligned} \tag{5}$$

where the dimensionless flow parameter through this dimensionless process can be obtained as

Name of Parameter	Dimensioless Parameter
Rotation	$\omega=\frac{\upsilon\Omega}{U_0^2}$
Second Grade fluid	$\alpha=\frac{\alpha_1 U_0^2}{\rho\upsilon^2}$
Modified Hartman number	$E=\frac{\pi\upsilon J_0 M_0}{8\rho U_0^3}$

3.1 Laplace Transform

Now, the momentum equation needs to be solved in order to obtain the velocity profiles of the fluid flow problem. The partial differential equation (PDE) in equation (4) needs to be transformed into an ordinary differential equation (ODE) by applying the Laplace transform, subject to the initial condition given in equation (5), yielding:

$$\frac{d^2\bar{F}}{dz^2}-\left(\frac{s+2i\omega}{\alpha s+1}\right)\bar{F}=-\frac{E}{s(\alpha s+1)}\exp(-lz) \tag{6}$$

and together with Laplace boundary condition

$$\begin{aligned} &\bar{F}(0,s)=0\,,\\ &\bar{F}(\infty,s)=0\,. \end{aligned} \tag{7}$$

Here, s is the Laplace transform variable. By applying the homogeneous and particular solutions subject to the boundary conditions in equation (7), the velocity in the Laplace domain can be obtained as:

$$\bar{F}(z,s)=\bar{F}_1(s)\times\bar{F}_2(z,s) \tag{8}$$

where,

$$\bar{F}_1(s) = \frac{a_5}{s - a_6},$$

$$\bar{F}_2(z,s) = \frac{1}{s}\cdot \exp\left(-\sqrt{a_1}\sqrt{\frac{s+2i\omega}{s+a_1}}\right) - \frac{1}{s}\exp(-lz),$$

in which

$$a_1 = \frac{1}{\alpha},\ \ a_2 = a_1 E,\ \ a_3 = l^2 - a_1,$$

$$a_4 = 2i\omega a_1 - a_1 l^2,\ \ a_5 = \frac{a_2}{a_3},\ \ a_6 = \frac{a_4}{a_3}.$$

3.2 Inverse Laplace Transform

Finally, to obtain the solution for the velocity profile, the inverse Laplace transform is applied to equation (8) using the method of compound functions.

$$F(z,t) = F_1(t) \times F_2(z,t) \tag{9}$$

and convolution theorem

$$F(z,t) = \int_0^t F_1(t-r) \times F_2(z,r)\,dr \tag{10}$$

which obtained as

$$F_1(t-r) = a_5 \exp\left(a_6 (t-r)\right)$$

$$F_2(z,r) = \exp\left(-z\sqrt{a_1}\right) - \exp(-lz) + \frac{z\sqrt{a_1 a_7}}{2\sqrt{\pi}} \int_0^r \int_0^\infty \frac{1}{u\sqrt{s}} \exp\left(-\frac{a_1 z^2}{4u} - a_1 s - u\right) \times I_1\left(2\sqrt{a_7 us}\right) du\,ds$$

where $a_7 = 2i\omega$. The skin friction of the flow problem is expressed as

$$\tau(z,t) = \left(1 + \alpha\frac{\partial}{\partial t}\right)\frac{\partial F}{\partial z}\bigg|_{z=0} \tag{11}$$

to determine the velocity gradient at the boundary layer of the Riga plate at $z = 0$, which significantly affects the fluid flow parameters, equation (10) is substituted into equation (11). The resulting expression is then utilized in the Response Surface Methodology (RSM) for statistical analysis to identify the most dominant parameters, as discussed in the following section.

4. RESULTS AND DISSCUSSION

In this section, the velocity profiles and skin friction results obtained from Eqs. (10) and (11) will be analyzed graphically using Mathcad and Minitab. Subsequently, the profiles corresponding to distinct values of each parameter will be examined in detail.

.

The effect of rotation on fluid velocity is clearly illustrated in Figure 3, which depicts the behavior of both primary and secondary velocities for two different rotation (ω) rates. Observations of the primary velocity show that an increase in the rotation rate leads to a significant decrease in velocity. This phenomenon aligns with the principles of rotating fluid dynamics, where the Coriolis force is a deflective force resulting from the rotating system which acts to resist the flow's original direction. This force becomes more dominant as the rotation rate increases, progressively slowing down the primary flow. Interestingly, although the primary velocity decreases, the Coriolis force directly drives the formation of secondary velocity. In a rotating system, the interaction between the primary velocity and the Coriolis force generates a perpendicular flow component known as secondary velocity. Thus, an increase in the rotation rate also results in a significant rise in the secondary velocity, as shown in the figure. However, within the range $4<z<5$, fluctuations in the velocity profile are observed, which are believed to be caused by disturbances in the magnetic field generated by the Riga plate. These disturbances affect the flow stability in that zone. Overall, the effect of rotation not only slows down the primary velocity through the influence of the Coriolis force but also triggers the development of secondary velocity, making the fluid flow more complex, comprehensive, and dynamic.

Meanwhile, the effect of the magnetic field generated by the Riga plate is illustrated in Figure 4 through the influence of the modified Hartmann number (E). Consistent with the observations in Figure 3, Figure 4 shows the velocity profiles for cases involving the Riga plate (E=1) and without the Riga plate (E=0) for both primary and secondary velocity components. It is evident from the figure that the presence of the Riga plate has a significant effect on increasing the fluid velocity. The fluid flowing through the Riga plate exhibits higher velocities compared to the flow without the Riga plate. As explained in the formulation section, the Riga plate generates a Lorentz force aligned with the direction of the fluid flow. In this context, the force is represented through the modified Hartmann number parameter. This Lorentz force acts as an additional driving mechanism that accelerates the fluid motion through electromagnetic thrust. Therefore, the fluid flow is influenced not only by the effect of rotation but also enhanced by the electromagnetic interaction produced by the Riga plate.

As been discussed earlier, the fluid investigated in this study is a second grade fluid, a type of non-Newtonian fluid that exhibits complex rheological behavior. This fluid is characterized by a key parameter, denoted as α, which plays a significant role in determining the flow behavior. The effect of the α parameter on velocity is shown in Figure 5, where both primary and secondary velocities display notable fluctuation patterns. For example, fluctuations in primary velocity are clearly visible within the range $3<z<4$, while the secondary velocity experiences significant changes around z=7. This pattern indicates the presence of both viscous and elastic characteristics within the fluid flow. As is well known, second grade fluids possess high viscosity and exhibit two main properties which are viscous and elastic. The flow behavior illustrated in the figure confirms that these properties interact dynamically which an initial increase in the α value leads to a decrease in velocity, which is later followed by an increase at a certain point. This transition reflects a shift from viscous dominance to an elastic response within the flow system. Overall, the α parameter not only influences the stability and velocity profiles but also highlights the transition of the fluid's physical nature from viscous to elastic behavior which is a critical phenomenon for understanding the flow mechanisms of second grade fluids in depth. Furthermore, the presence of the Riga plate also slightly alters the fluid's motion and viscosity behavior.

Next, the fluctuation behavior observed in Figure 5 is also reflected in Figure 6 when there is an increase in the time parameter (t). However, the pattern of velocity variation in this case shows some differences. Unlike the case involving the second grade fluid parameter, the velocity in Figure 6 initially increases before undergoing a significant decrease. This phenomenon indicates that, at the early stage, the fluid experiences substantial acceleration due to the combined effects of the magnetic field from the Riga plate and the system's rotation. These two factors act together to drive the fluid motion, resulting in an increase in velocity. However, as the effect of the fluid's viscosity begins to dominate, particularly due to the viscoelastic nature of the second grade fluid, the velocity starts to decrease. This transition signifies a shift in dominance from external forces to the fluid's intrinsic properties. This observation further reinforces the finding that all parameters involved in the system which including the magnetic field, rotation rate, time parameter, and rheological properties of the fluid, interact in a complex and comprehensive manner to influence the flow dynamics. Additionally, analysis of the entire figure shows that the velocity reaches a steady state when the axial value $z \geq 10$, where velocity changes become nearly zero. This demonstrates that the flow system achieves full stability at a certain distance along the channel which an important characteristic for managing and predicting fluid behavior in practical applications.

The change in the contour plot of skin friction (SF) with respect to E and ω is illustrated in Figure 7. The parameter α is set to 5.5. As depicted, the highest SF value (greater than 0.075) is represented by the darkest green, while the lowest SF value (0.00) is indicated by the brightest green. It is observed that the lowest SF values are obtained at the lowest ω values (between 1 and 3), regardless of the value of E. However, when ω exceeds 3, an increase in E is also observed, resulting in a more significant SF level. When both ω and E exceed 7, located on the right side of the graph, the highest SF value (dark green) is reached. It can be concluded that the SF value is strongly dependent on ω, and is also influenced by E, particularly when both parameters are high.

Next, the contour plot comparing α and ω with respect to the SF value at a fixed E is presented in Figure 8. It is clearly shown that at low ω values (between 1 and 3), low SF values are obtained regardless of the magnitude of α, indicating that ω has a significant effect within this range. A notable increase in SF is observed when ω exceeds 5, although α remains within low to medium values (between 1 and 6). It is further observed that the increase in SF occurs more gradually when both ω is high and α exceeds a value of 7. The highest SF values are achieved when a high ω is combined with a low α. This suggests that a non-linear interaction between ω and α plays a critical role in determining the SF value when EEE is maintained at 5.5.

In contrast, the diagram in Figure 9 is shown with two primary color gradients which are blue and green where dark blue represents the lowest SF value, while dark green indicates the highest. It is observed that the SF value increases as the E value increases and the α value decreases. The lowest SF values, including negative values (represented in blue), are displayed in the upper left region of the plot, corresponding to low E and high α. A nearly linear gradient of SF values is observed, forming an oblique contour pattern extending from the top left to the bottom right.

From the observation of these graphs, it can be concluded that the rotational parameter ω is more dominant compared to the modified Hartmann number E and the second-grade fluid parameter α.

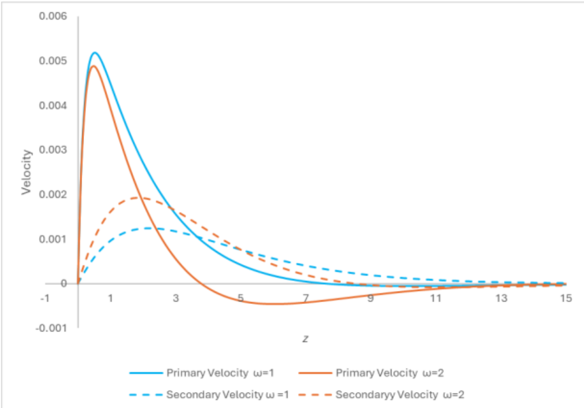

Fig. 3. Primary (a) and secondary (b) velocity profile for different values of rotation parameter.

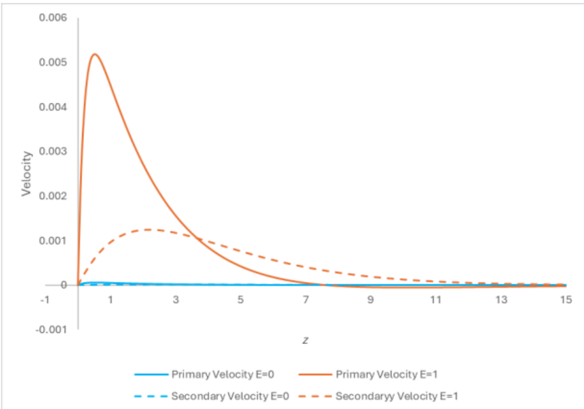

Fig. 4. Primary (a) and secondary (b) velocity profile for different values of magnetic Hartman number parameter.

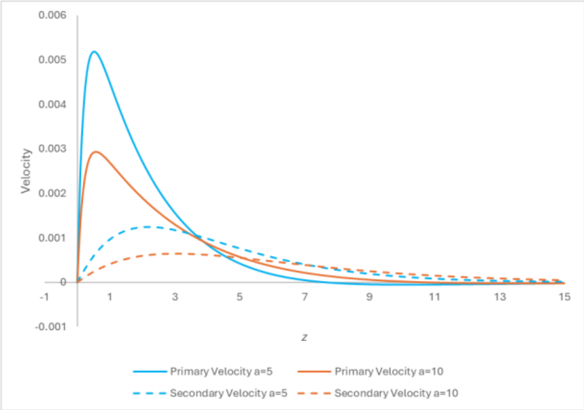

Fig. 5. Primary (a) and secondary (b) velocity profile for different values of second grade fluid parameters.

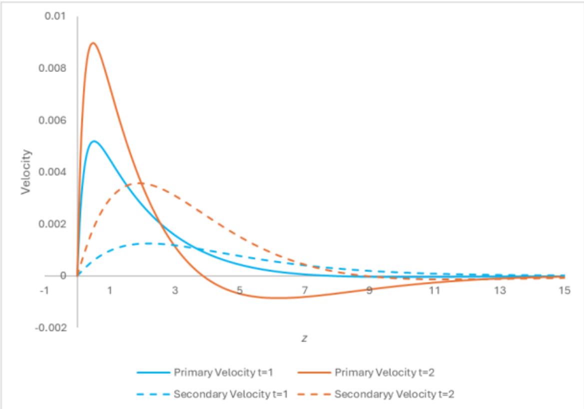

Fig. 6. Primary (a) and secondary (b) velocity profile for different values of suction parameters.

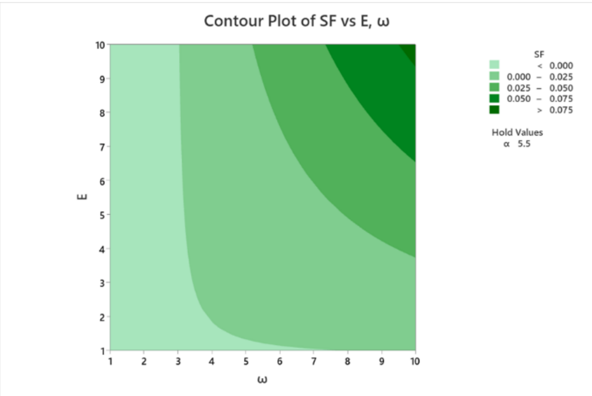

Fig. 7. Statistical analysis on contour plot for skin friction between rotation and modified Hartman number.

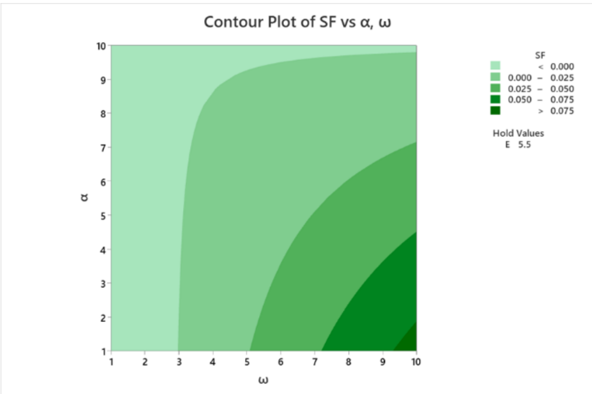

Fig. 8. Statistical analysis on contour plot for skin friction between rotation and second grade fluid parameter.

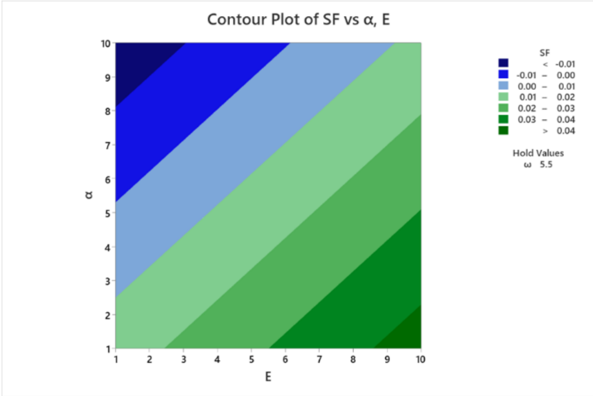

Fig. 8. Statistical analysis on contour plot for skin friction between modified Hartman number and second grade fluid parameter.

5. CONCLUSION

In this paper, the exact analytical and statistical solutions for the flow of a rotating second-grade fluid over an infinite vertical Riga plate are investigated.

1. The dimensional momentum partial differential equation is formulated based on the Boussinesq approximation, relevant literature, the physical configuration and assumptions presented in Figure 2, along with selected initial and boundary conditions.
2. Suitable dimensionless variables are introduced to obtain the dimensionless form of the equations and boundary conditions.
3. The Laplace and inverse Laplace transforms are applied to derive the velocity profiles of the flow problem.
4. Skin friction is analyzed based on the velocity profiles using Response Surface Methodology (RSM) for statistical analysis.
5. An increase in the rotation parameter reduces the primary velocity and increases the secondary velocity due to the Coriolis force.
6. The velocity is higher in the presence of the Riga plate (Modified Hartmann number E=1) and lower in its absence (E=0).
7. The velocity profiles of the second-grade fluid and the time parameter show similar fluctuating behavior due to viscous, elastic, and magnetic effects.
8. Statistical analysis shows that the parameter rotation ω is the most dominant.
9. The findings of this study not only provide theoretical insights but also offer potential applications in engineering and industrial processes involving fluid flow control and heat transfer enhancement.

For future research, this problem can be verified, and the experimental results analyzed, as shown in [29]. Furthermore, it can also be considered for medical applications, as the properties of this second-grade fluid can be categorized as those of blood flow through arterial stenosis [30], with rotational effects induced by a rotatable medical device [31].

6. REFERENCES

[1] Mohamad, A. Q., Khan, I., & Shafie, S. (2019). Magnetic effects on second grade fluid flow due to non coaxial rotation of a disk through a porous medium with double diffusion. *Journal of Magnetics*, *24*(3), 379-391.

[2] Zin, N. A. M., Mohamad, A. Q., Khan, I., & Shafie, S. (2016, October). Heat and mass transfer of unsteady MHD free convection flow of second grade fluid with Newtonian heating. In *AIP Conference Proceedings* (Vol. 1775, No. 1). AIP Publishing.

[3] Ismail, Z., Khan, I., Mohamad, A. Q., & Shafie, S. (2015, May). Second grade fluid for rotating MHD of an unsteady free convection flow in a porous medium. In *Defect and Diffusion Forum* (Vol. 362, pp. 100-107). Trans Tech Publications Ltd.

[4] Mohamad, A. Q., Lim, Y. J., Khan, I., Zin, N. A. M., Shafie, S., & Ismail, Z. (2017, September). Analytical solution for unsteady second grade fluid in presence of non-coaxial rotation. In *Journal of Physics: Conference Series* (Vol. 890, No. 1, p. 012040). IOP Publishing.

[5] Hayat, T., & Hutter, K. (2004). Rotating flow of a second-order fluid on a porous plate. *International Journal of Non-Linear Mechanics*, *39*(5), 767-777.

[6] Hayat, T., Nadeem, S., Siddiqui, A. M., & Asghar, S. (2004). An oscillating hydromagnetic non-Newtonian flow in a rotating system. *Applied mathematics letters*, *17*(5), 609-614.

[7] Hayat, T., Nadeem, S., Asghar, S., & Siddiqui, A. M. (2005). Effects of Hall current on unsteady flow of a second grade fluid in a rotating system. *Chemical Engineering Communications*, *192*(10), 1272-1284.

[8] Hayat, T., Fetecau, C., & Sajid, M. (2008). Analytic solution for MHD transient rotating flow of a second grade fluid in a porous space. *Nonlinear Analysis: Real World Applications*, *9*(4), 1619-1627.

[9] Khan, I., Farhad, A., Sharidan, S. and Norzieha, M. (2010). Exact solutions for Accelerated flows of Rotating Second Grade Fluid in a Porous Medium. World Applied Sciences Journal. 9: 55–68.

[10] Imran, M. A., Imran, M., & Fetecau, C. (2014). MHD oscillating flows of rotating second grade fluids in a porous medium. *Communications in Nonlinear Science and Numerical Simulation*, *2014*, 1-12.

[11] Zafar, A. A., Vieru, D. U. M. I. T. R. U., & Akhtar, S. H. A. H. R. A. Z. (2015). Magnetohydrodynamics of rotating fractional second grade fluid in porous medium. *Journal of Prime Research in Mathematics*, *10*, 45-58.

[12] Mohamad, A. Q., Khan, I., Jiann, L. Y., Shafie, S., Isa, Z. M., & Ismail, Z. (2017). Heat transfer on rotating second grade fluid through an accelerated plate. *Malaysian Journal of Fundamental and Applied Sciences*, *13*(3), 219-223.

[13] Pantokratoras, A. (2011). The Blasius and Sakiadis flow along a Riga-plate. *Progress in Computational Fluid Dynamics, An International Journal*, *11*(5), 329-333.

[14] Reyaz, R., Mohamad, A. Q., Yeou, J. L., Khan, A., & Shafie, S. (2024). Mxene and Strontium Titanate Hybrid Casson Nanofluid with CMC Base via the Caputo-Fabrizio Fractional Derivative over a Vertical Riga Plate. *Semarak International Journal of Nanotechnology*, *1*(1), 45-64.

[15] Reyaz, R., Mohamad, A. Q., Jiann, L. Y., & Shafie, S. (2023). Analytical Treatment for Accelerated Riga Plate on Fractional Caputo-Fabrizio Casson Fluid. *CFD Letters*, *15*(4), 114.

[16] Reyaz, R., Mohamad, A. Q., Lim, Y. J., Saqib, M., & Shafie, S. (2022). Analytical solution for impact of Caputo-Fabrizio fractional derivative on MHD casson fluid with thermal radiation and chemical reaction effects. *Fractal and Fractional*, *6*(1), 38.

[17] Anjum, A., Mir, N. A., Farooq, M., Javed, M., Ahmad, S., Malik, M. Y., & Alshomrani, A. S. (2018). Physical aspects of heat generation/absorption in the second grade fluid flow due to Riga plate: application of Cattaneo-Christov approach. *Results in Physics*, *9*, 955-960.

[18] Rasool, G., Zhang, T., & Shafiq, A. (2019). Second grade nanofluidic flow past a convectively heated vertical Riga plate. *Physica Scripta*, *94*(12), 125212.

[19] Rasool, G., & Wakif, A. (2021). Numerical spectral examination of EMHD mixed convective flow of second-grade nanofluid towards a vertical Riga plate using an advanced version of the revised Buongiorno's nanofluid model. *Journal of Thermal Analysis and Calorimetry*, *143*(3), 2379-2393.

[20] Waqas, H., Khan, S. U., Shehzad, S. A., Imran, M., & Tlili, I. (2020). Activation energy and bioconvection aspects in generalized second-grade nanofluid over a Riga plate: a theoretical model. *Applied Nanoscience*, *10*, 4445-4458.

[21] Al-Zubaidi, A., Nazeer, M., Hussain, F., & Saleem, S. (2025). Numerical study of squeezing flow past a Riga plate with activation energy and chemical reactions: Effects of convective and second-order slip boundary conditions. *Waves in Random and Complex Media*, *35*(3), 5933-5946.

[22] Gangadhar, K., Kumari, M. A., & Chamkha, A. J. (2022). EMHD flow of radiative second-grade nanofluid over a Riga Plate due to convective heating: Revised Buongiorno's nanofluid model. *Arabian Journal for Science and Engineering*, *47*(7), 8093-8103.

[23] Shatanawi, W., Abbas, N., Shatnawi, T. A., & Hasan, F. (2023). Heat and mass transfer of generalized fourier and Fick's law for second-grade fluid flow at slendering vertical Riga sheet. *Heliyon*, *9*(3).

[24] Khashi'ie, N. S., Zokri, S. M., Kasim, A. R. M., Waini, I., & Zainal, N. A. (2022). Insight into hybrid nanofluid induced by a Riga plate: investigation on second grade fluid model. *Waves in Random and Complex Media*, 1-18.

[25] Nadeem, S., Ishtiaq, B., Almutairi, S., & Ghazwani, H. A. (2022). Impact of Cattaneo–Christov double diffusion on 3d stagnation point axisymmetric flow of second-grade nanofluid towards a riga plate. *International Journal of Modern Physics B*, *36*(29), 2250205.

[26] Wahid, N. S., Mustafa, M. S., Arifin, N. M., Khashi'ie, N. S., & Pop, I. (2025). Hybrid nanofluid radiative flow across a permeable convective moving surface with heat generation: Numerical

and statistical approach. *Neural Computing and Applications*, *37*(5), 2911-2923.

[27] Abu Bakar, S., Wahid, N. S., Md Arifin, N., & Pop, I. (2025). Optimization of heat transfer on Jeffrey ternary nanofluid flow with slip conditions and heat generation by response surface methodology. *Multiscale and Multidisciplinary Modeling, Experiments and Design*, *8*(2), 1-17.

[28] Hakeem, A. A., Ragupathi, P., Saranya, S., & Ganga, B. (2020). Three dimensional non-linear radiative nanofluid flow over a Riga plate. *Journal of Applied and Computational Mechanics*, *6*(4), 1012-1029.

[29] Rahman, T., & Islam, A. (2020). Determination of Flow Characteristics and Performance Analysis of the Non-Rotating & Rotating Cylinder.

[30] Dey, S., Ibtida, T., Roy, C. K., & Sakib, N. (2020). Difference between non-Newtonian Carreau and Casson blood viscosity models to predict hemodynamics in idealized eccentric arterial stenosis: large eddy simulation modelling.

[31] Noranuar, W. N. I. N., Mohamad, A. Q., & Shafie, S. (2025). Heat and mass transfer on MHD rotating Casson Blood-CNTs nanofluid flow in porous channel for biomedical applications. Computers in Biology and Medicine, 193, 110371.